INTRAOPERATIVE VISUALIZATION OF ANATOMICAL STRUCTURES IN MASSIVE BLEEDING USING INFRARED IMAGES

A.V. Medievsky [1] *, A.G. Zotin [2], K.V. Simonov [3], T.V. Cherepanova [1], A.S. Kruglyakov [3]

[1] Krasnoyarsk State Medical University named after Professor V.F. Voyno-Yasenetsky, 1 Partizan Zheleznyaka st., 660022, Krasnoyarsk, Russian Federation – amedievsky@yandex.ru
[2] Reshetnev Siberian State University of Science and Technology, 31 Krasnoyarsky Rabochy pr., 660037, Krasnoyarsk, Russian Federation – zotin@sibsau.ru
[3] Institute of Computational Modelling of the SB RAS, 50/44 Akademgorodok, 660036, Krasnoyarsk, Russian Federation – simonovkv@icm.krasn.ru

Commission II, WG II/8

KEY WORDS: Endoscopy, Near Infrared, NIR, Segmentation, Shearlet Transform, Color Coding, Neurosurgery, Intraoperative Bleeding.

ABSTRACT:

One of the most dangerous complications during brain surgery is bleeding. Hemostasis can be difficult due to the lack of visibility caused by blood filling the surgical wound. To restore the visibility of the surgical area it is proposed to use NIR-camera data and Shearlet transform with color-coding algorithms. At the same time it is also assumed to conduct brightness characteristics enhancement of images (frames) and segmentation of biological tissues of interest. NIR beams are able to penetrate deeper into tissues than visible light and NIR is also absorbed to a greater extent by hemoglobin than by surrounding tissues. The blood has a significantly higher absorption coefficient of NIR rays in the range from 800 nm to 1050 nm in comparison with the absorption coefficient of the same spectrum by the tissues involved during the operation. Due to this effect there is the potential to detect structures of interest despite bleeding in the wound cavity. During experimental study it was found that it becomes possible to visualize all tissues that are at a depth of up to 3 mm. Use of BCET algorithm with the mask for processing made it possible to improve the image contrast from 34.20% to 198.73% depending on the depth of biological structures. In case of model images processing the best average accuracy of determining ROI contours taking into account depth was 0.961 ± 0.021 according Dice similarity coefficient.

1. INTRODUCTION

For the speedy recovery of patients minimally invasive operations are now being carried out everywhere. With this method the size of the surgical field may not exceed a few centimeters. The small size of the cavity does not allow the surgeon to fully carry out the necessary maneuvers at the proper speed. In the case of the surgeon's actions with possible massive bleeding the existing view from the endoscope will be largely blocked.

One of the main problems with bleeding is the difficulty of determining its source. This may be caused by poor visibility when the entire operational access is filled with blood. At the moment there is no video endoscopic equipment that could visualize the tissues of interest through the massive volume of blood shed. In such cases the surgeon has to work almost blindly.

To solve this problem it is proposed to use special endoscopic equipment with a built-in near infrared sensor. It is proposed to process images using a set of algorithms for noise reduction and improvement of brightness characteristics as well as Shearlet transform using color coding of objects of interest.

The work is aimed at the study of algorithms that provide better visualization of biological structures during surgical operations with massive bleeding. The proposed computational technique will contribute to the fastest detection of the source of bleeding and the implementation of high-quality hemostasis.

The study assumes the use of algorithmic support for the study of low-contrast images and the detection of blood vessels by selected patterns. The processing technique consists in applying BCET algorithms, gamma correction, histogram equalization as well as algorithms based on Retinex variation and Shearlet transform including color coding of objects of interest.

As a part of the experimental study it is also supposed to evaluate the change in the contrast ratio when using various algorithms for improving the brightness characteristics, depending on the depth of the biological tissue. The proposed computational technique makes it possible to obtain the maximum contrast image in the minimum amount of time which makes it possible to make appropriate estimates in real time.

The development of the proposed system (equipment and technique) will make it possible to achieve a reduction in the time spent to stop bleeding, save a larger volume of vital structures and also avoid possible postoperative complications.

* Corresponding author

2. MATERIALS AND METHODS

2.1 Formulation of the problem and NIR - Endoscopy

Blood has a red color due to the presence of hemoglobin protein in erythrocytes. Its main functions are the binding and transport of oxygen molecules. Depending on the number of bound oxygen molecules the spectrum of absorbed light changes.

The leveling of differences in absorption coefficients can be achieved by using near infrared light (NIR) with a wavelength of 800 nm (Dervieux et al., 2020). NIR beams are able to penetrate deeper into tissues than visible light (Shourav et al., 2021) and NIR is also absorbed to a greater extent by hemoglobin than by surrounding tissues (Wang et al., 2007).

The blood has a significantly higher absorption coefficient of NIR rays in the range from 800 nm to 1050 nm in comparison with the absorption coefficient of the same spectrum by the tissues involved during the operation (Calabro, 2020). Due to this effect there is the potential to detect structures of interest despite bleeding in the wound cavity.

Using infrared rays as a source of illumination the image will be formed as follows: one part of the electromagnetic radiation will be absorbed by the blood elements and the other part will reach the tissues of the surgical wound. Further, the reflected rays will again pass through the elements of blood. Those rays that do not experience absorption will fall on the endoscope lens which will form a two-dimensional image.

To illuminate NIR beams of deep tissues it is proposed to use a medical endoscope with two fiber optic bundles. This will allow the device to be kept as small as possible and obtain images without the delay typical for digital endoscopes.

We note some features that force the use of optical fiber. During the experiment it is necessary to obtain two types of images (in the normal spectrum and in the NIR). At the same time it is not rational to install two cameras on the distal end of the endoscope since this will significantly increase its size. The small size of the fiber-optic endoscope is its main advantage in solving the stated problem.

In (Buenconsejo A.L. et al., 2019) a scheme of an endoscope is described, the tip diameter of which does not exceed 900 μm. This allows it to be used in combination with other surgical instruments without the need to expand the surgical field. This feature is important when stopping bleeding with an electrocoagulator in hard-to-reach places.

In order to validate the reliability of the method of visualization of biological tissues at the time of bleeding a model of the surgical field was prepared. For this purpose a histological preparation of the human brain was used placed in a transparent plastic cup with venous blood.

The images for the study were obtained using an IP camera with a 5 MP Sony CMOS 335E matrix. Its peculiarity is rather high light sensitivity. This matrix is capable of capturing both visible and infrared ranges. Therefore, for the reliability of the results, both images were taken on the same matrix. The change in shooting modes was carried out by using an optical filter that cuts off rays with a wavelength of more than 740 nm. Figure 1 demonstrates the differences in imaging structures of interest in the visible and near-infrared spectrum.

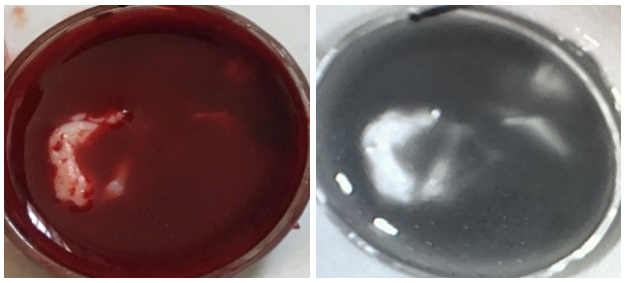

a b

Figure 1. Example of the model surgical field images: a) visible spectrum; b) near infrared spectrum.

The use of NIR cameras (b) makes it possible to view structures that are deeper than with conventional imaging (a).

To confirm the reliability of the results a comparison was made of the silhouette of the blood vessel before and after the development of bleeding. Figure 2 shows images of the thoracic aorta of a mouse in the visible spectrum (Figures 2a) and NIR spectrum (Figures 2b). The upper row of Figure shows the state before bleeding in the lower one during bleeding.

We compared the object of interest in Figure 2b of the second row and the silhouette of the vessel from Figure 2a of the first row. In this case the contours coincided which means that in Figure 2b after the development of bleeding the aorta is visualized and not interpreted as artifact. Visualization in the NIR range allows to see deeper structures.

Currently there are several approaches that allow the neurosurgeon to maintain visibility and perform hemostasis in the event of intraoperative bleeding.

Operations using endoscopic equipment allow the use of such techniques as dry-field maneuver (Turhan, 2018; Oertel et al., 2018) and small-chamber irrigation technique (SCIT) (Manwaring et al., 2014).

The dry-field maneuver method is based on the aspiration of cerebrospinal fluid from the ventricles which helps to identify and coagulate the source of bleeding. The SCIT method uses additional fluid to irrigate the surgical field.

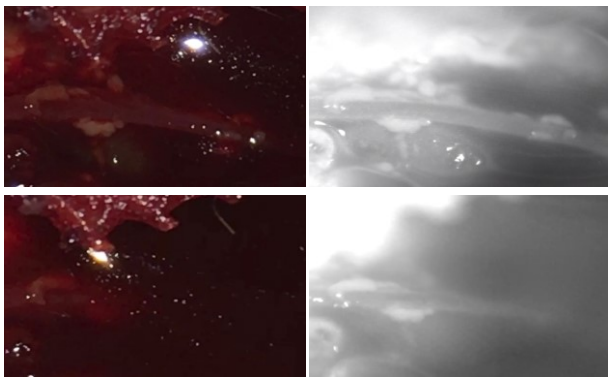

a b

Figure 2. The thoracic part of the mouse aorta: a) image in the visible spectrum; b) image in the NIR spectrum.

The solution flushes out red blood cells directly in front of the camera which clears the field of view of the endoscope. At the same time the effective use of methods is possible only when working with minor bleeding.

2.2 Description of the processing method

After receiving the images they are processed in two stages: pre-processing and the formation of a color representation. Pre-processing includes noise reduction and brightness correction. To suppress noise it was decided to use an adaptive median filter with weight coefficients.

To perform the correction of brightness characteristics the algorithms such as Balance Contrast Enhancement Technique (BCET) (Zotin et al., 2019), Gamma correction, Histogram equalization (Patel et al., 2013) as well as algorithms based on the Retinex variation (Zotin, 2020) were chosen.

When using variations of Retinex the output image was formed by applying the BCET algorithm to the response, stretching the range taking into account the standard deviation and linear stretching with a multiplier. The formation of the color representation is based on the use of the Shearlet transform and color coding of objects of interest (Zotin et al., 2020).

3. EXPERIMENTAL STUDIES

For prompt and adequate evaluation of the visible operating area by the surgeon a computational method for image processing has been developed. The methodology includes procedures designed to correct the brightness characteristics, produce noise reduction as well as improve the contrast and detail of the tissues of objects of interest.

Evaluation of the effectiveness of the proposed algorithms was carried out through expert analysis. All presented versions of the original images were studied by specialists and comparisons were made (Figure 3).

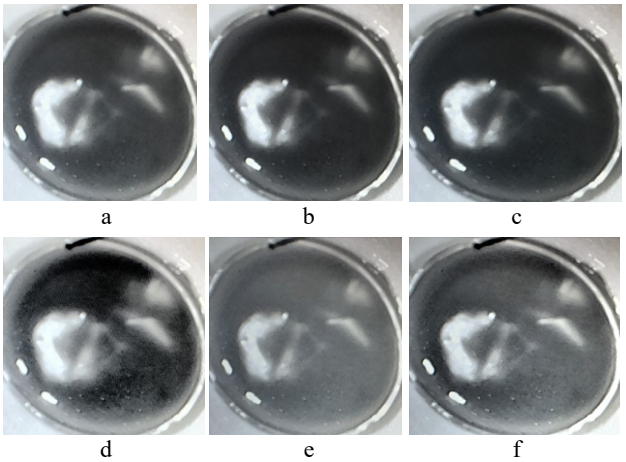

Figure 3. Example of image contrasting of original image: a) BCET; b) BCET mean100; c) gamma correction 0.7; d) Histogram equalization; e) Retinex with BCET; f) Retinex with SD scaling.

The camera generates images with size 1920×1080. The observability of objects was assessed by a specialist in the process of filling the model of the surgical field with blood. At the same time, a reference description of objects of interest was formed.

Based on a comparative analysis between the contrasting options used, three most successful ones can be distinguished. The results are shown in Figure 3b, Figure 3c and Figure 3d. These images were selected for further processing (Figure 4) using the proposed method based on the modified algorithm of Shearlet transform and color coding of objects of interest.

Figure 4a shows the processing of the original image based on the application of the Shearlet transform and color coding. This allows to get the desired idea about the object of interest. At the same time we note that in Figure 4a the image of the first row does not correctly reflect the morphology of biological structures. The image of the second row (Figure 4a) complicates the analysis of the morphology of the underlying tissues.

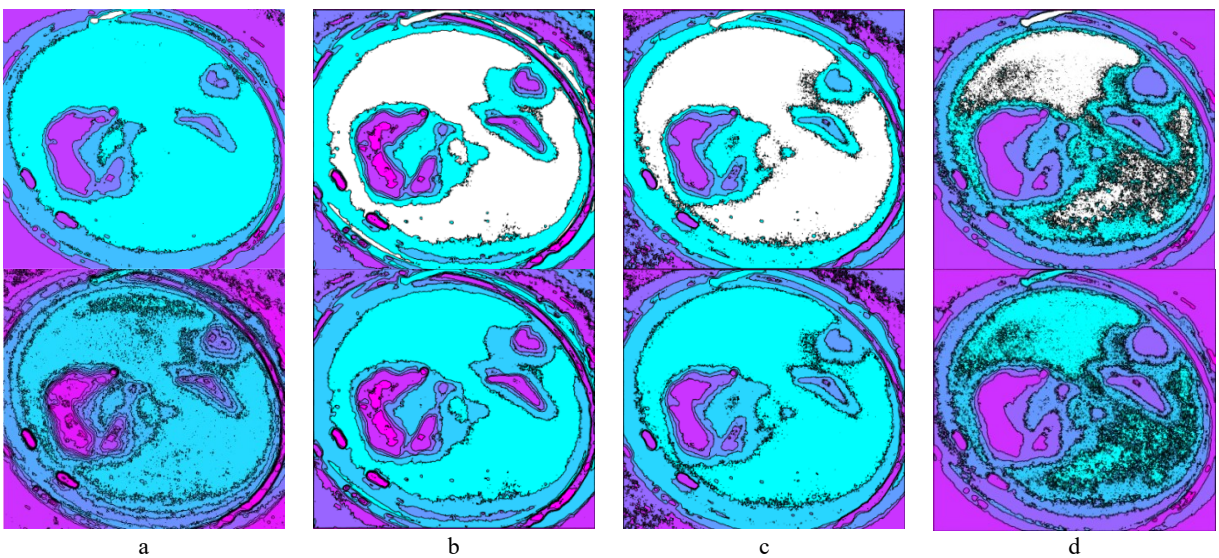

Figure 4. Results of applying the Shearlet transform and color coding technique: a) processing of the original image; b) color coding Figure 3b; c) color coding Figure 3c; d) color coding Figure 3d.

All other images of the first and second rows shown in Figure 4b, Figure 4c and Figure 4d have a rich color gradient. This allows to visualize in detail the relief of brain tissue. But the most adequate in terms of perception is the image of the first row in Figure 4b. This option combined all the necessary characteristics: a more complete gradient, morphology accuracy and good contrast with the background.

After establishing the operability of the technique an additional experiment was conducted to determine the effectiveness of each processing method through the use of a ruler. For the experiment a ruler was specially developed a feature of which is the ability to determine the depth of each section of the brain preparation.

The ruler is designed in the form of a ladder in which each step is responsible for its depth and one step is equal to a depth change of exactly 1 mm. The ruler has 6 steps due to the small size of the studied biological preparation. The first step is on the surface and characterizes the 0 mm mark and the sixth step therefore the -5 mm mark (Figure 5).

In accordance with the brightness of the ruler pixels we can set the depth of one of the brain regions (Figure 6). If a random pixel taken from the lower part of the brain preparation corresponds in brightness to the pixel located on a step equal to 3 mm then we can conclude that this area of the brain is also at a depth of 3 mm.

As part of the application of the BCET algorithm processing was performed in two ways. The first option took into account the data of the entire image and the second only the mask of the observed scene (Masked BCET). In this case the region that outside the boundaries of the object of interest defined by the mask was considered as dark field (minimal brightness intensity).

During processing data were obtained under various conditions (more than 30 variants). Figure 7 shows the best results from the point of view of experts (medical specialists).

Figure 7 visually shows the improvement in the contrast of all images. The most successful variants of processing demonstrate the maximum difference in the brightness characteristics of the background and the brain tissue. These images were obtained by applying methods such as: Masked BCET; Masked BCET mean 100; Histogram equalization and Gamma correction 1.75.

The best variants of preliminary processing were selected for further processing using Shearlet transform and color coding. Examples of processing results are shown in Figure 8.

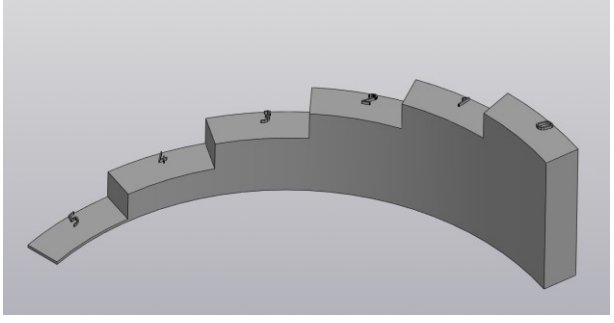

Figure 5. 3D model of the ruler.

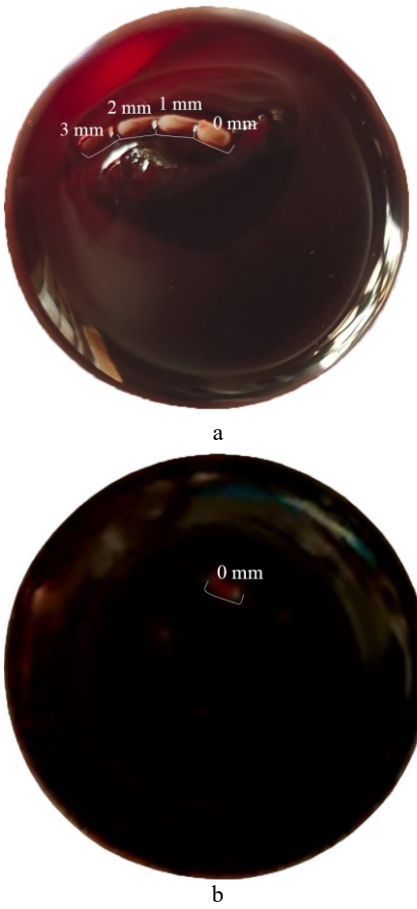

Figure 6. Brain preparation with a ruler in the visible spectrum: a) before filling with blood; b) after filling with blood.

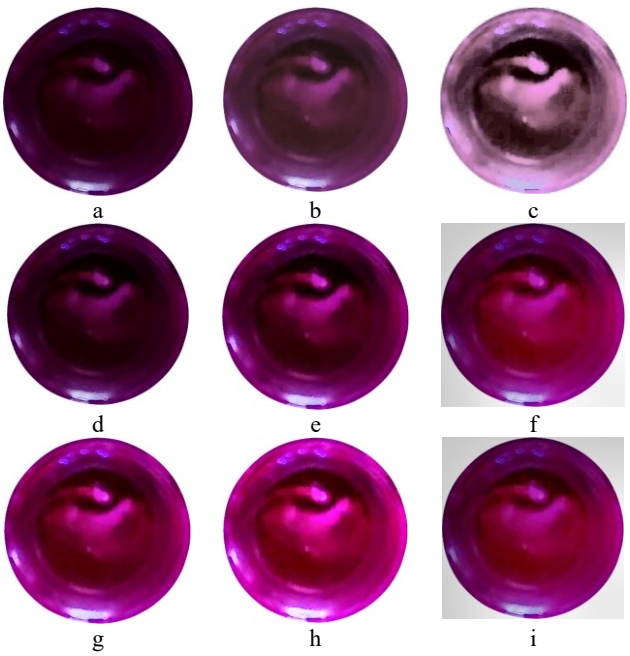

Figure 7. Examples of brightness characteristics enhancement of NIR image: a) Original; b) Gamma correction 1,75; c) Histogram equalization; d) BCET mean 100; e) BCET; f) Retinex with BCET scaling; g) Masked BCET mean 100; h) Masked BCET; i) Retinex with SD scaling.

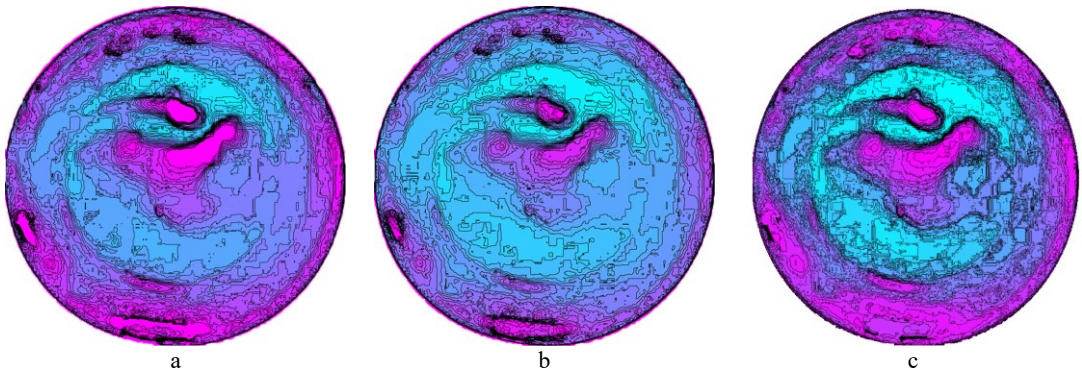

a b c

Figure 8. Examples of applying Shearlet transformation and color coding to the images: a) Masked BCET; b) Masked BCET mean 100; c) Histogram equalization.

By visual assessment, they equally well separate the studied areas from the light turquoise background. Due to color coding, biological structures become easier to perceive. This allows much faster detection of a damaged blood vessel.

4. DISCUSSION: EVALUATION OF THE EFFECTIVENESS OF THE APPLIED METHODOLOGY

To assess the effectiveness of the applied contrasting techniques the contrast ratios for individual locations at various depths were calculated. 100 pixels were randomly selected at each visible level of the ruler: 0 mm; -1 mm; -2 mm; -3 mm and their relative brightness was determined.

Next the relative brightness of the background represented only by blood was determined in comparison with which the contrast of the images was determined. The location of the selected pixels was the same for the entire series of shots.

The arithmetic mean values of the contrast ratios for each depth are shown in Table 1. Contrast ratios were determined using algorithms established by the Web Content Accessibility Guidelines where the lowest value is 1 and the highest is 21 (Hristov et al., 2022).

Comparative characteristics of contrasting methods with respect to the original image are shown in Table 2. It follows from it that it is impossible to select the best contrasting option since no method has the largest percentage at all depths at once.

The Histogram Equalization method has the highest percentage of improvement at a depth of -1 to -2 mm, but at a depth of -3 mm the Masked BCET method is most effective which improves the contrast of the original image by 34.2%.

The use of Shearlet transform and color coding made it possible to further improve the contrast of images (Table 3).

Masked BCET combined with Shearlet transform improved the region of interest (ROI) visibility by 10.73% compared to using Masked BCET alone; Shearlet transform with pre-processing by Masked BCET mean 100 – by 11.21%.

The Shearlet transform combined with preliminary processing based on Histogram equalization where the least improvement was expected we received the largest increase in ROI visibility by 96.33%. In combination with the original enhancement 16.23% this gives a 2-fold improvement – 112.56%.

The estimation of region of interest (ROI) determination from the results of the Shearlet transform and color coding for different depths was carried out using the Dice similarity coefficient metric.

The evaluation was performed relative to the maps formed by the expert during the filling of the brain preparation (imitation of surgical field) with blood. The average Dice similarity coefficient values for model images are shown in Table 4.

Processed Images	Depth			
	0 mm	-1 mm	- 2 mm	- 3 mm
Original	2,042	1,209	1,071	1,035
Gamma correction 1,25	2,563	1,327	1,124	1,064
Gamma correction 1,5	3,095	1,499	1,215	1,113
Gamma correction 1,75	3,506	1,688	1,303	1,198
Histogram equalization	10,698	5,882	2,166	1,203
BCET	4,540	1,815	1,252	1,109
Masked BCET	6,100	2,919	1,798	1,389
BCET среднее 100	2,499	1,300	1,092	1,042
Masked BCET mean 100	5,412	2,177	1,481	1,244
Retinex BCET Scaling	3,451	1,906	1,389	1,163
Retinex SD Scaling	3,165	1,818	1,366	1,156

Table 1. Contrast ratios of the studied elements depending on their location depth.

Processed Images	Depth			
	0 mm	-1 mm	- 2 mm	- 3 mm
Original	2,042	1,209	1,071	1,035
Gamma correction 1,25	25,51	9,76	4,95	2,80
Gamma correction 1,5	51,57	23,99	13,45	7,54
Gamma correction 1,75	71,69	39,62	21,66	15,75
Histogram equalization	423,90	386,52	102,24	16,23
BCET	122,33	50,12	16,90	7,15
Masked BCET	198,73	141,44	67,88	34,20
BCET среднее 100	22,38	7,53	1,96	0,68
Masked BCET mean 100	165,03	80,07	38,28	20,19
Retinex BCET Scaling	69,00	57,65	29,69	12,37
Retinex SD Scaling	55,00	50,37	27,54	11,69

Table 2. The enhancement of the use of various methods in comparison with original in percentages.

Base processed Images	Coefficient of contrast, units	Improvement, %
Histogram equalization	2.20	112,56%
Masked BCET	1.50	44,93%
Masked BCET mean 100	1.36	31,40%

Table 3. Image contrast ratio after Shearlet transform and color coding.

Processed Images	Depth			
	0 mm	- 1 mm	- 2 mm	- 3 mm
Histogram equalization	0.984	0.979	0.971	0.954
Masked BCET	0.973	0.965	0.961	0.934
Masked BCET mean 100	0.971	0.961	0.948	0.889

Table 4. Average values of Dice similarity coefficient.

5. CONCLUSION

This stage of the study showed that the proposed method for pre-processing images can improve the accuracy of determining the position of the desired areas by 2.8-3.9% and the selection of the corresponding boundaries by 2.3-4.8%. In this case the average accuracy of determining contours in model images was 0.961 ± 0.021 according to Dice similarity coefficient.

A computational technique has been developed for visualizing the surgical field during massive bleeding. A technique is proposed for using an NIR endoscope with contrasting algorithms, Shearlet transform and color coding in minimally invasive surgery.

As part of the experimental study the substantiation, testing of methods and combinations of algorithms was carried out. A feature of the developed approach is that it can be used both as an independent method of tissue visualization and in conjunction with existing ones.

It was found that when using preprocessing methods for brightness characteristics enhancement it becomes possible to visualize all tissues that are at a depth of up to 3 mm. With the help of Masked BCET it was possible to improve the image contrast from 34.20% to 198.73% depending on the depth of biological structures.

REFERENCES

Buenconsejo, A.L., Hohert, G., Manning, M., Abouei, E., Tingley, R., Janzen, I., McAlpine, J., Miller, D., Lee, A., Lane, P., MacAulay, C., 2019. Submillimeter diameter rotary-pullback fiber-optic endoscope for narrowband red-green-blue reflectance, optical coherence tomography, and autofluorescence in vivo imaging. *Journal of biomedical optics*, 25 (3), 1-7.

Calabro, K.W., 2020. Modeling Biological Tissues in LightTools.

Dervieux, E., Bodinier, Q., Uhring, W., Theron, M., 2020. Measuring hemoglobin spectra: searching for carbamino-hemoglobin. *Journal of Biomedical Optics*, 25, 1-15.

Hristov, H., Glushkova, T., Cheresharov, S., Stoeva, M., 2022. A model for designing accessible color and contrast for users with visual deficiency and color blindness. *IEEE 11th International Conference on Intelligent Systems (IS)*, 1-7. Warsaw, Poland.

Manwaring, J.C., El Damaty, A., Baldauf, J., Schroeder, H.W., 2014. The small-chamber irrigation technique (SCIT): a simple maneuver for managing intraoperative hemorrhage during endoscopic intraventricular surgery. *Neurosurgery*, 10 (3), 375-379.

Oertel, J., Linsler, S., Csokonay, A., Schroeder, H., Senger, S., 2018. Management of severe intraoperative hemorrhage during intraventricular neuroendoscopic procedures: the dry field technique. *Journal of neurosurgery*, 131 (3), 931-935.

Patel, O., Maravi, Y., Sharma, S., 2013. A Comparative Study of Histogram Equalization Based Image Enhancement Techniques for Brightness Preservation and Contrast Enhancement. *Signal & Image Processing : An International Journal (SIPIJ),* 4 (5), 11-25.

Shourav, M.K., Choi, J., Kim, J.K., 2021. Visualization of superficial vein dynamics in dorsal hand by near-infrared imaging in response to elevated local temperature. *Journal of biomedical optics*, 26 (2), 026003.

Turhan, T., 2018. Dry-field maneuver for controlling the massive intraventricular bleeding during neuroendoscopic procedures. Child's nervous system. *Journal of the International Society for Pediatric Neurosurgery*, 34 (3), 541-545.

Wang, L., Leedham, G., Gho, S., 2007. Infrared imaging of hand vein patterns for biometric purposes. *IET Computut. Vis*., 1 (3), 113-122.

Zotin, A., Hamad, Y., Simonov. K., Kurako, M., 2019. Lung boundary detection for chest X-ray images classification based on GLCM and probabilistic neural networks. *Procedia Computer Science*, 159, 1439-1448.

Zotin, A.G., 2020. Fast algorithm of image enhancement based on multi-scale Retinex. *Int. J. Reasoning-based Intelligent Systems*, 12 (2), 106-116.

Zotin, A., Simonov, K., Kapsargin, F., Cherepanova, T., Kruglyakov, A., 2020. Tissue Germination Evaluation on Implants Based on Shearlet Transform and Color Coding. In: Editor, Favorskaya, M., Jain, L. *Computer Vision in Advanced Control Systems-5*, 175, 265-294. Springer, Cham.